Taylor & Francis
Taylor & Francis Group

RESEARCH PAPER/REPORT

🔓 OPEN ACCESS   ✓ Check for updates

Periodontitis pathogen *Porphyromonas gingivalis* promotes pancreatic tumorigenesis via neutrophil elastase from tumor-associated neutrophils

Qin Tan[a]*, Xiao Ma[b,c]*, Bing Yang[a], Ye Liu[d], Yibin Xie[e], Xijun Wang[a], Wei Yuan[b], and Jie Ma[a]

[a]Center of Biotherapy, Beijing Hospital, National Center of Gerontology; Institute of Geriatric Medicine, Chinese Academy of Medical Sciences, Beijing, P.R. China; [b]State Key Laboratory of Molecular Oncology, National Cancer Center/National Clinical Research Center for Cancer/Cancer Hospital, Chinese Academy of Medical Sciences and Peking Union Medical College, Beijing, P.R. China; [c]Department of Clinical Laboratory, Beijing Friendship Hospital, Capital Medical University, Beijing, P.R. China; [d]The Key Laboratory of Geriatrics, Beijing Institution of Geriatrics, Beijing Hospital, National Center of Gerontology, National Health Commission, Institute of Geriatric Medicine, Chinese Academy of Medical Sciences, Beijing, P.R. China; [e]Department of Pancreatic and Gastric Surgery, National Cancer Center/National Clinical Research Center for Cancer/Cancer Hospital, Chinese Academy of Medical Sciences and Peking Union Medical College, P.R. China

ABSTRACT

Intratumor microbiome shapes the immune system and influences the outcome of various tumors. *Porphyromonas gingivalis* (*P. gingivalis*), the keystone periodontal pathogen, is highly epidemically connected with pancreatic cancer (PC). However, its causative role and the underlining mechanism in promoting PC oncogenesis remain unclear. Here, we illustrated the landscape of intratumor microbiome and its bacterial correlation with oral cavity in PC patients, where *P. gingivalis* presented both in the oral cavity and tumor tissues. When exposed to *P. gingivalis*, tumor development was accelerated in orthotopic and subcutaneous PC mouse model, and the cancerous pancreas exhibited a neutrophils-dominated proinflammatory tumor microenvironment. Mechanistically, the intratumoral *P. gingivalis* promoted PC progression via elevating the secretion of neutrophilic chemokines and neutrophil elastase (NE). Collectively, our study disclosed the bacterial link between periodontitis and PC, and revealed a previously unrecognized mechanism of *P. gingivalis* in PC pathophysiology, hinting at therapeutic implications.

Introduction

Pancreatic cancer (PC) remains the most aggressive cancer worldwide, with a 5-year survival rate of 8%.[1] Although previous studies revealed multiple epidemic risk factors of PC, the pathophysiological mechanisms are still unclear.[2] Periodontitis, with oral microbiota dysbiosis, has been increasingly associated with systematic diseases, including diabetes,[3] cardiovascular disease,[4] and cancer.[5] Recent accumulating evidence suggests the possible "mouth–gut axis" of pathogenesis in gastrointestinal disease,[6] who considered the digestive tract could be "inoculated" from the oral cavity.[7] Notably, clinical observations have demonstrated that the prevalence of PC significantly increases in chronic periodontitis patients.[8,9] *Porphyromonas gingivalis* (*P. gingivalis*), a keystone oral-resident

periodontal pathogen, was reported not only being involved in the oncogenesis of several gastrointestinal cancers,[10] such as esophageal cancer[11] and colorectal cancer,[7] but also being epidemically correlated with PC.[12–14] These observations suggest the potential causative link between periodontitis and PC might be mediated by *P. gingivalis*. However, how *P. gingivalis* may intervene in the pathophysiological process of PC remains elusive.

Intratumor microorganisms make up the important part of tumor microenvironment (TME), affecting the *in situ* tumorigenesis, progression and therapeutic responses.[15] The pancreas has once considered as a sterile organ, where the presence of bacteria and fungi within pancreatic cancer tissues have been discovered.[16] Significantly, microbial ablation attenuated tumor growth in pancreatic

cancer mouse model, with an increase of innate and adaptive immune suppression,[17,18] suggesting that microorganisms could shape the residing immune landscapes of pancreatic cancer.[19] And thus, we speculated periodontitis-derived *P. gingivalis* may contribute to PC tumorigenesis via intervening in the process of immune TME.

Neutrophils are the initial line of innate immune defense of exogenous pathogens.[20] It is widely accepted that *P. gingivalis* infection always causes skewed host inflammation responses in chronic periodontal disease, which accounts for an abundant accumulation with neutrophils.[21,22] Neutrophils have three major roles to trap microorganisms: phagocytosis, degranulation, and neutrophil extracellular traps (NETs).[20] While the neutrophil elastase (NE), one of the major mediators of NETs' formation, has recently been reported with in-turns effects on tumorigenesis.[23,24] Nevertheless, whether intratumoral *P. gingivalis* could shape the inflammation response in PC via neutrophils-derived NE has not been described.

In this study, we dissected the tumor microbiome ecology of PC patients and its correlation with clinical features. We also found the different bacterial profiles between saliva and tumor tissues from PC patients, but shared some common microbiota distributions, including *P. gingivalis*. Consistent with this observation, experimental studies revealed that *P. gingivalis* from oral cavity could be inoculated and enriched in the cancerous pancreas, as well as promoting PC progression in mouse tumor models. *P. gingivalis*-infected PC tumors recruit tumor-associated neutrophils in microenvironment, with the elevated release of neutrophilic chemokines and NE. Furthermore, targeting the recruitment of neutrophils and NE release obtained remarkable protection against PC and enhanced antitumor immunity. Collectively, these data suggested that by recruiting tumor-associated neutrophils and activated NE releasing, *P. gingivalis* generates a pro-inflammatory microenvironment, which ultimately contributes to the progression of pancreatic neoplasms. Our study disclosed the connection between periodontitis and PC through the understanding of how *P. gingivalis* influences the inflammatory responses inside tumor and hinted the corresponding therapeutic strategies for PC patients with *P. gingivalis* invasion.

Result

The tumorous pancreas has an abundant intratumor microbiome

To explore the human intrapancreatic microbiome composition, we performed 16s Ribosomal RNA Gene Sequencing (16s rRNA) on resected cancer tissue and matched normal adjacent tissues (NAT), employed from 20 pancreatic patients (Clinical characteristics are shown in Sup Table S1). Refraction curves of each sample were found approached saturation, indicating the adequate sequencing depth and the abundant presence of bacteria (Sup Figure S1a). We first sought to determine the landscape of the microbial composition between PC tumor and their NAT, which presented a similar community at various taxonomic levels (Figure 1a, Sup Figure S1b). 150 distinct classes were detected in human PC tumor and NAT. *Gammaproteobacteria* (31.2%), *Bacteroidia* (14.1%), *Clostridia* (12.8%), *Bacilli* (12.2%), *Alphaproteobacteria* (11.7%) were most prevalent in all PC specimens (Figure 1b, Sup Table S2). Although the overall microbial composition was relatively similar, we explored the differential taxonomic prevalence in tumors and their NAT. By visualizing the operational taxonomic units (OTUs) abundance at the genus level with comparison heatmap, 44 genera were found significantly different between PC and NAT ($p<0.05$, Figure 1c and Sup Table S3).

Importantly, we further evaluated the potential correlation between microbiome composition of PC tumor tissues and common clinical parameters. Selective enrichment of genera were predicted significant correlation with smoking status, differentiation status, serum CA19-9 level as well as cancer stage, while no association with cancer position was observed (Figure 1d). *Herbaspirillum, Brucella, Allorhizobium–Neorhizobium–Pararhizobium–Rhizobium*, belonging to the *Proteobacteria* phylum, are the highly enriched genera in never smokers, which are also specifically exploited in moderately differential PC patients. While *Treponema* (*Spirochaetota* phylum), *Pseudorhodoplanes*, and *Sphingomnas* (*Proteobacteria* phylum) were also both markedly presented in CA19-9 normal and early-stage PC patients. Besides, the probiotics *Lactobacillus* and *Lactococcus* aggregated more in CA19-9 normal patients (Figure 1d). To extend our
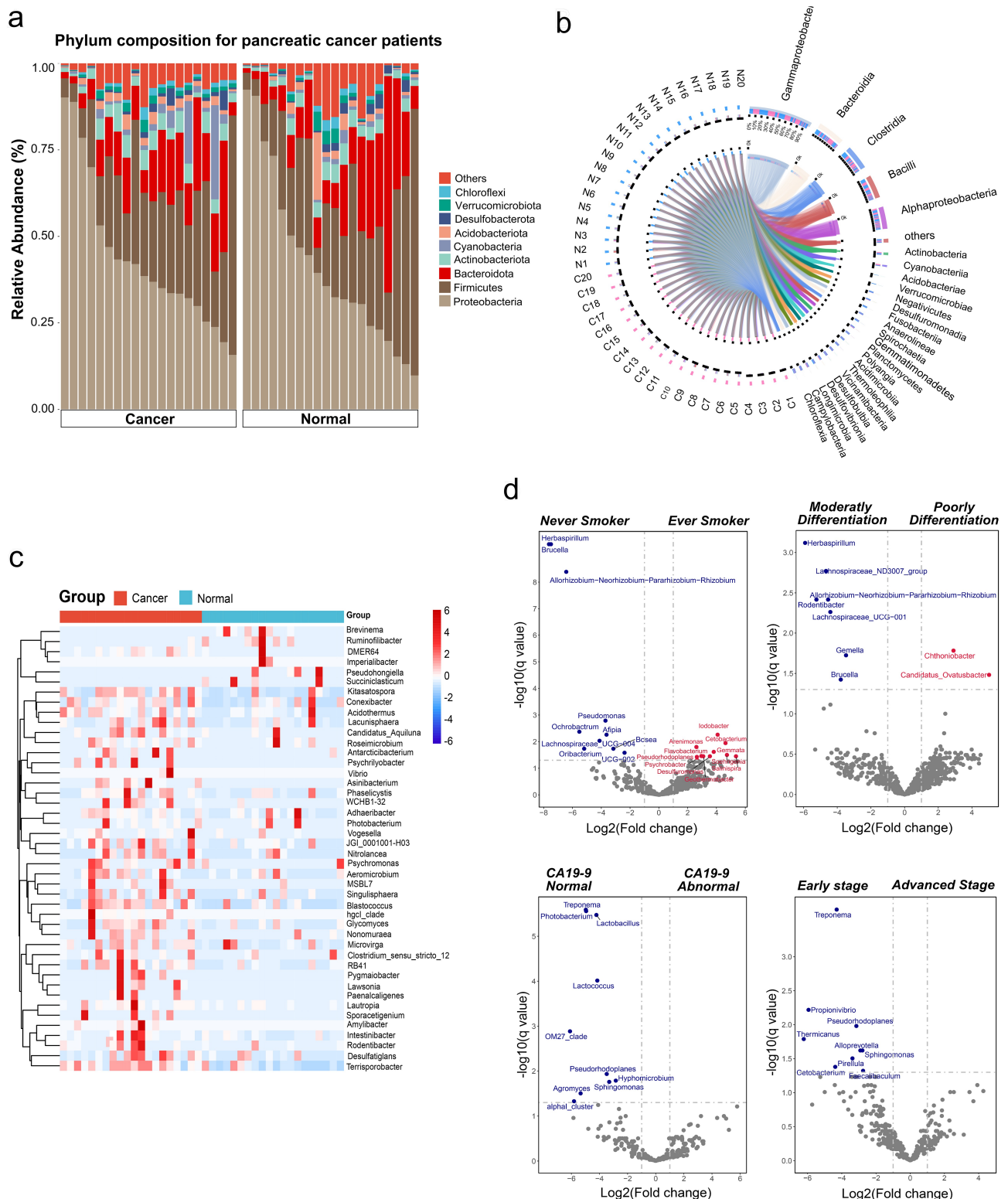
Figure 1. Intratumor microbiota composition of cancer tissues and NAT in pancreatic cancer patients. (a) Bar plots of top ten enriched phylum taxonomies in the cancerous pancreas and normal adjacent tissues (NAT). Relative abundance is plotted for each patient. Normal means NATs. (b) Circos map visualizing the most abundant classes in tumors and their NATs; Others combined the relative abundance of classes <0.01. (c) Heatmap of the most differentially abundant genus taxa between pancreatic cancer and NAT. Difference with *p*<0.05 were selected (Wilcoxon signed-rank test). The left panel shows Hierarchical Ward-linkage clustering based on Pearson correlation coefficients of the genera. (d) Volcano plot demonstrating the enriched bacteria in cancer samples with multiple clinicopathologic factors, the relatively significantly increased and decreased bacteria were colored in red or blue, respectively. (Wald test, FDR-corrected *q*-value <0.05, and fold change >2). CA19-9 normal means blood CA19-9 level less than 37 U/mL, CA19-9 abnormal means the level over 37 U/mL; Early stage includes stage I, II patients, advanced stage includes stage III, IV patients.

understanding of microbiome diversity, we assessed alpha and beta-diversity by various indices or principal component analysis (PCA)/principal coordinate analysis (PCoA), respectively, while no statistical difference was detected (Sup Figure S1c-S1d).

Tumor microbiome communities are partially shared with the oral cavity

Considering the relationship between oral pathogens and prospective high risks of pancreatic cancer,[9–11] we then interrogated bacterial membership in oral wash samples from newly enrolled PC patients (Oral (cancer), n = 21), compared with those in resected PC tissues (Cancer, n = 20). At the phylum level, the intratumor and oral microbiota of PC patients were dominated by *Firmicutes, Protebacteria* and *Bacteroidota* (Sup Figure S2a). Notably, *Protebacteria* compromised only 5.53% of oral bacteria, while increased into 44.32% abundance in the cancerous pancreas (Sup Figure S2a). We then explored that the certain genera composition in both oral and intratumor of PC patients, where *Pseudomonas, Herbaspirillum* and *Sphingomonas* were the topmost enriched *Protebacteria* in PC, whereas *Neisseria, Haemophilus* and *Aggregatibacter* were more abundant *Protebacteria* in the oral cavity (Sup Figure S2b). To extend the understanding of the shared microbiome communities, we compared the possible shifted species in the oral cavity, cancerous pancreas as well as NAT. *P. gingivalis* was exhibited among all groups by visualizing the shared species (Figure 2a, Sup Figure S2c). Altogether, these data revealed the potential relationship of bacterial migration between the oral cavity and *in situ* PC tissues.

P. gingivalis is aggregated in cancerous pancreas tissues than normal adjacent tissues

To further demonstrate the presence of *P. gingivalis* within *in situ* PC samples, we estimated the relative abundance of *P. gingivalis* in cancer tissue and NAT at species level. As shown in Figure 2b, *P. gingivalis* was more abundant in the cancerous pancreas, rather than NAT ($p < 0.05$). To confirm the intratumoral location of *P. gingivalis* in pancreatic cancer tissue, we

externally validated in 26 paired tumor and NAT formalin-fixed paraffin-embedded (FFPE) samples by performing ribosomal RNA (rRNA) fluorescence *in situ* hybridization (FISH), using universal bacterial probe EUB338 and *P. gingivalis* oligonucleotide probe PGOI. As expected, the FISH analysis of universal bacteria confirmed the presence of bacterial DNA in approximately all PC samples, and the number of *P. gingivalis* FISH plaque was significantly enriched in pancreatic cancer tissues compared to NAT sections (35.3 ± 56.3 vs 1.6 ± 3.7 plaques/per spot, $p < 0.001$, Figure 2c,d). These data indicate that *P. gingivalis* is localized and enriched in the cancerous pancreatic tissues, which may suggest the potential pathogenic role in PC tumorigenesis.

P. gingivalis promotes pancreatic tumorigenesis in C57BL/6 mice

Considering *P. gingivalis* was detected in both oral cavity and pancreatic cancer tissues, we postulated that *P. gingivalis* could shift from the oral cavity to the pancreas and promote pancreatic cancer progression. To determine whether *P. gingivalis* can migrate into the pancreas, calcein AM-labeled *P. gingivalis* was oral gavaged in C57BL/6 mice every other day for 2 weeks. Flow cytometry and FISH confirmed the presence of *P. gingivalis* in the pancreas and feces via bacteria-gavaging, compared with un-gavaged mice (Sup Figure S3a-S3c). To confirm the hypothesis of tumorigenesis, murine PC cell lines Pan02 were orthotopically implanted into the pancreas, during the *P. gingivalis*-gavaged migration model. The mice were sacrificed after implanting cancer cells for 3 weeks, then tumor weight and tumorigenesis features of the pancreas were explored after 5 weeks of treatment (Figure 3a). As shown in Figure 3b,c, *P. gingivalis*-gavaged mice developed significantly higher tumor burden compared with vehicle-gavaged mice ($p < 0.05$). Besides, *P. gingivalis*-treated tumor showed increased cell proliferation, as evidenced by Ki-67$^+$ cells ($53.2 \pm 9.74\%$ vs $29.8 \pm 13.8\%$, $p < 0.001$, Figure 3d,e), which are largely in line with the *in vivo* observation. Given that *P. gingivalis* was enriched in human pancreatic cancer tissues and accelerated PC progression in mice, we hypothesized that *P. gingivalis* could also
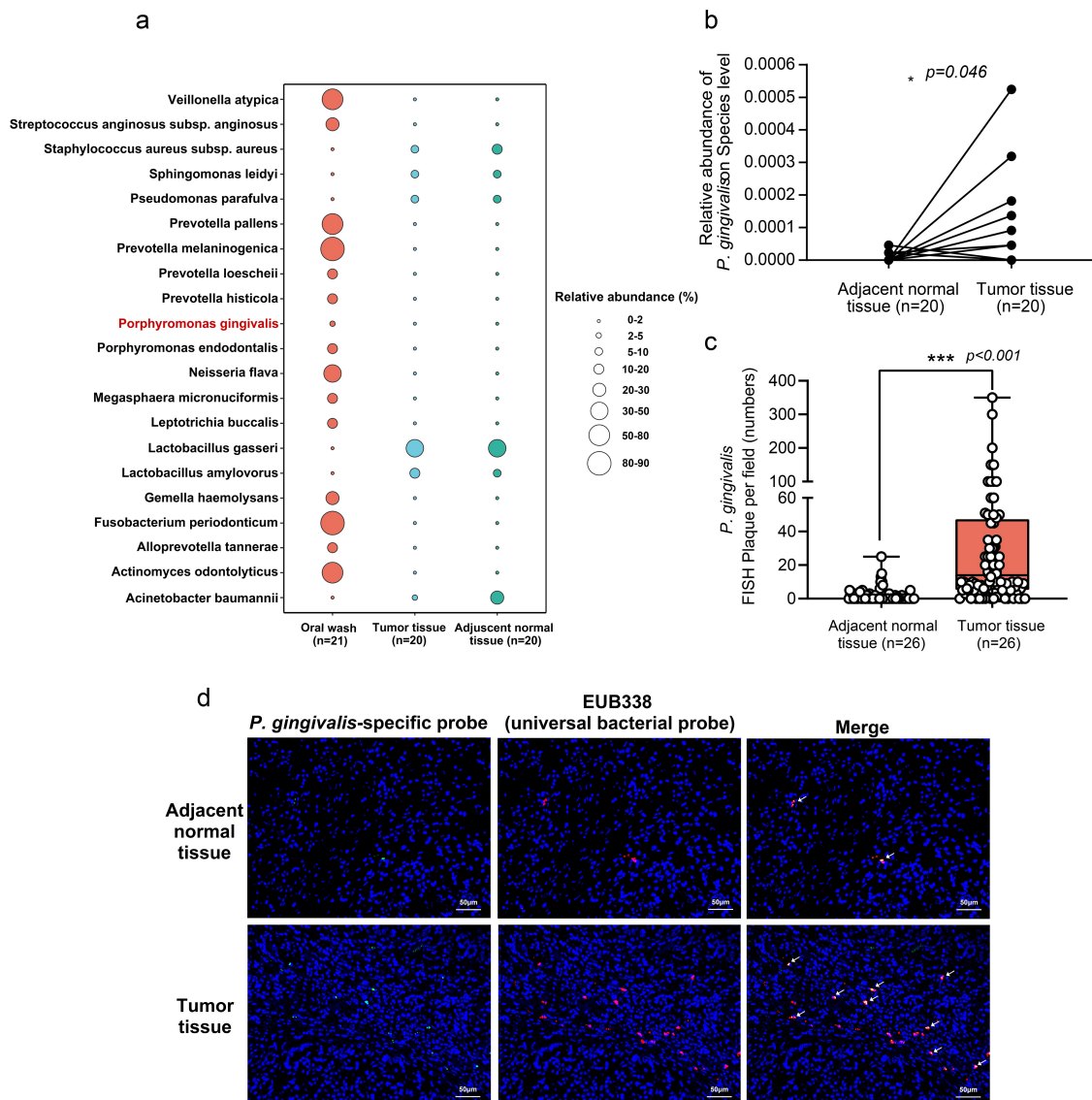
Figure 2. *P. gingivalis* is aggregated in cancerous pancreas tissues than normal adjacent tissues. (a) The shared species of top 20 enriched bacteria and *P. gingivalis*, presented both in the oral wash, tumor tissue and NAT samples, in alphabetical order. Circle size indicated the prevalence level. *P. gingivalis* was highlighted in red. (b) The relative abundance of *P. gingivalis* in tumor tissues versus NAT is plotted based on 16s rRNA sequencing (*$p<$ 0.05). (c) Quantitative analysis of *P. gingivalis* FISH plaques in (d) from 26 representative paired-PC tumor tissues and NAT, at least three 200× fields per slide were randomly selected for analysis (***$p<$ 0.001). The p-value was calculated by two-tailed paired t-test. (d) Representative fluorescence *in situ* hybridization (FISH) images of *P. gingivalis* in human PC tumor tissues and NAT samples using Alexa 488-conjugated *P. gingivalis*-specific probe (PGOI, green) and Cy3-conjugated universal bacterial 16s rRNA-directed oligonucleotide probe (EUB338, red). (Arrows, *P. gingivalis* colonization, scale bar 50 μm).

be localized within the tumor in PC mice. The FISH analysis showed *P. gingivalis* was obviously presented in *P. gingivalis*-treated tumor, compared with control tumor (14.5 ± 17.3 vs 0.6 ± 0.8 plaques/per spot, $p<$ .01, Figure 3f,g). These data indicated the possible oral-pancreas migration of *P. gingivalis*, which could accelerate pancreatic tumorigenesis and be enriched in tumor tissue of PC mice.

P. gingivalis modifies the inflammatory tumor microenvironment (TME)

To investigate the potential mechanism of *P. gingivalis* in inducing pancreas tumorigenesis, we first examined the morphological features of the tumor sections by hematoxylin and eosin (H&E) stains. *P. gingivalis* treated-tumor showed the obviously increased necrosis with more
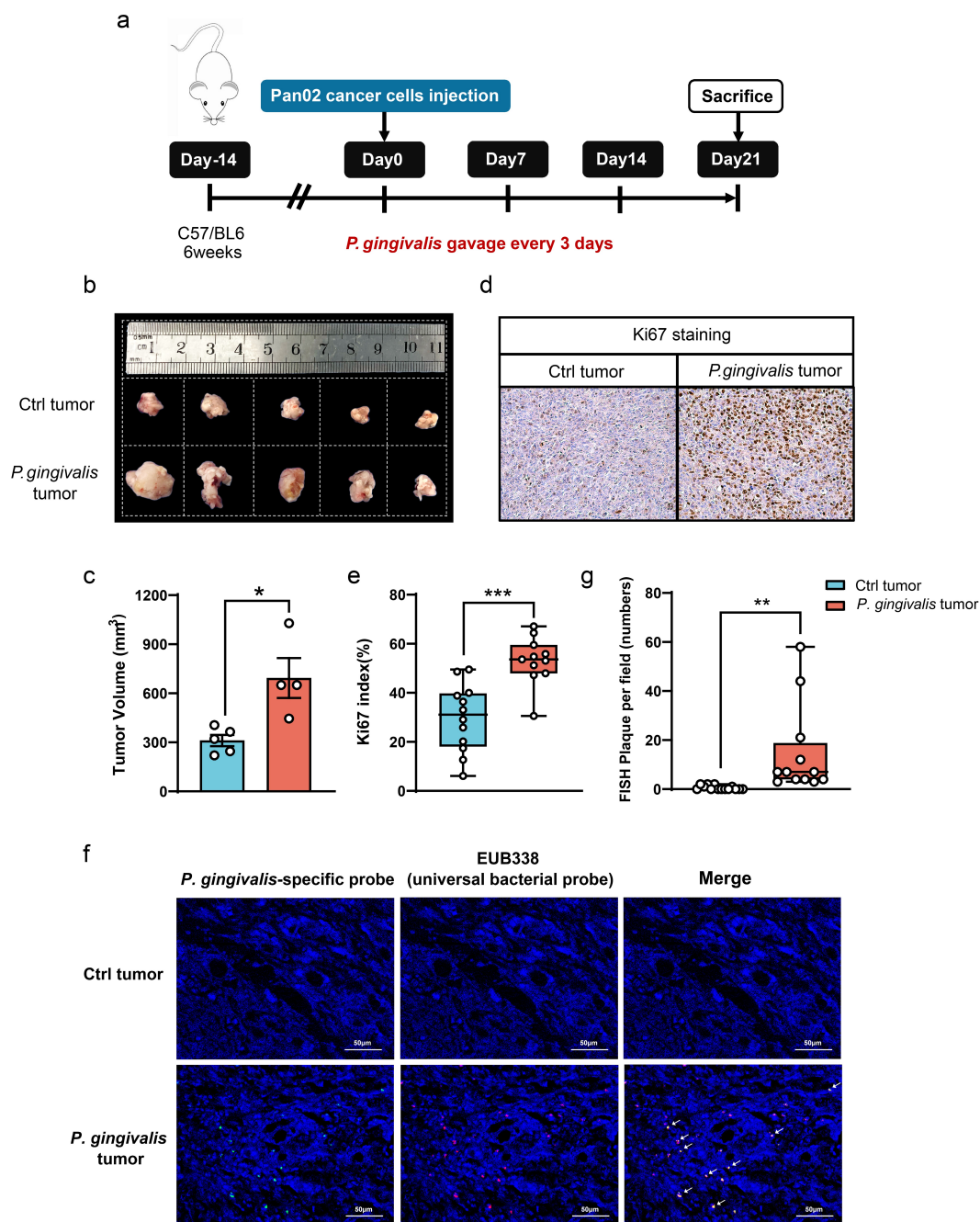
Figure 3. *P. gingivalis* promotes pancreatic tumorigenesis in C57/BL6 mice. (a) Schematic diagram of *P. gingivalis* administration to C57BL/6 mice with orthotopic pancreatic cancer. Male C57/BL6 mice aged 6 weeks were randomly divided into two groups, *P. gingivalis* was administered to mice via oral-gavaging every 3 days in the orthotopic Pan02 tumor model; control mice were oral gavaged with vehicle. Sacrificed at day 21 after Pan02 cell inoculation (n = 5 mice/group). (b) Representative *in situ* images of Pan02 tumors form orthotopic PC mice, oral gavaged with *P. gingivalis* or vehicle. ctrl tumor, vehicle-treated control tumor. *P. gingivalis* tumor, *P. gingivalis* oral-gavaged tumor. (c) The tumor volume (length × width^2 × 0.5) of *P. gingivalis* or vehicle-treated PC mice. *p< 0.05. (d) Representative immunohistochemistry images showing Ki67$^+$ cells of tumors in PC mice, after *P. gingivalis* or vehicle gavage (200×). (e) Quantitative analysis of Ki67$^+$cells in (D) per 200× field, at least three fields per slide were randomly selected. (f) Representative FISH detection of *P. gingivalis* in *P. gingivalis*-treated PC mice, using Alexa 488-conjugated *P. gingivalis*-specific probe (green) and Cy3-conjugated universal bacterial EUB338 probe, red (arrows, *P. gingivalis* colonization, 200×). (g) Quantitative analysis of FISH plaques in (F), at least three 200× fields per slide were randomly selected. Three independent experiments were repeated with similar results. (The mean ± SEM is shown. *p< 0.05, **p< 0.01, ***p< 0.001, two-tailed unpaired *t*-test).

infiltration of inflammatory immune cells compared with untreated tumor (necrosis area: 28.9 ± 15.3% vs 0.7 ± 0.4%, $p < 0.01$, Figure 4a upper), which were confirmed as enrichment of neutrophils by immunohistochemical (IHC) assessment of myeloperoxidase (MPO) (H-score: 79.7 ± 30.7 vs 23.9 ± 16.0, $p < 0.001$, Figure 4a bottom). Thus, we intended to explore the effect of *P. gingivalis* on the tumor immune landscape in PC. By assessing the composition of tumor-infiltrating immune cells using multi-colored flow cytometry, we also observed significant enrichment

of neutrophils (24.3 ± 8.85% vs 8.28 ± 2.17%, $p < 0.05$), interestingly, which showed a great decrease of CD8+ cytotoxic T cells (23.47 ± 6.05% vs 34.1 ± 8.62%, $p < 0.01$, Figure 4b), while no statistical changes in CD4+ T cells and monocytes (Sup Figure S4a). We next deeply characterized the TME characteristics of the cancerous pancreas by mRNA sequencing. In total, 353 differentially expressed genes (DEGs) were significantly upregulated and 557 DEGs were downregulated in *P. gingivalis*-treated tumor tissues compared with control tumor, clustered by expression levels
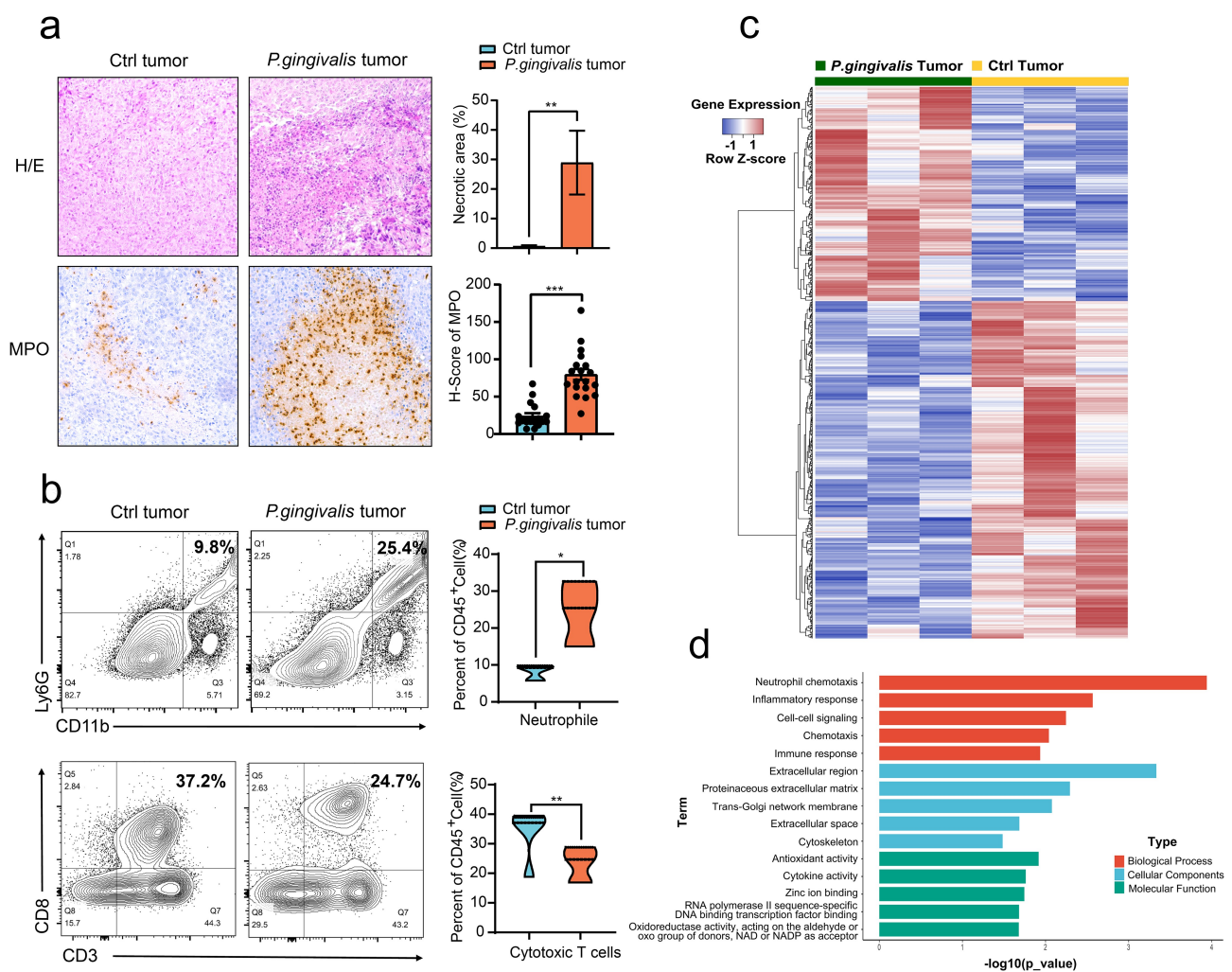

Figure 4. *P. gingivalis* modifies the inflammatory tumor microenvironment (TME). (a) Representative images of H&E histological staining and immunohistochemistry of myeloperoxidase (MPO) in PC tumor tissues after *P. gingivalis* or vehicle gavage (200×). The necrosis areas and the H-score of MPO were calculated, bar plot shows the quantitative result, at least three fields per slide were randomly selected (n = 5, **$p < 0.01$, ***$p < 0.001$, two-tailed unpaired *t*-test). (b) Representative flow cytometric analysis of neutrophils and CD8+ cytotoxicity T cells in *P. gingivalis* or vehicle-treated groups, gated in CD45+ cells. The percentages were plotted (n = 5, *$p < 0.05$, **$p < 0.01$, two-tailed unpaired *t*-test). (c) Heatmap showing the differentiated expressed genes (DEGs) of tumor tissues in PC mice response to *P. gingivalis* or vehicle gavage, measured by mRNA sequencing analysis (n = 3, DEGs: $p < .05$, log$_2$fold change >1, one-tailed Student's *t*-test). (d) Most significant gene ontology (GO) terms linked with upregulated genes in *P. gingivalis*-gavaged PC mice.

(Figure 4c,p<0.05, fold change >2, full genes were listed in Sup Table S4). Among these, significant gene ontology (GO) terms linked to upregulated and downregulated genes were identified (Figure 4d and Sup Figure S4b), where the most upregulated genes were functionally related to biological pathways of neutrophil chemotaxis, inflammatory response, cell–cell signaling, chemotaxis and immune responses in *P. gingivalis*-mediated mice (Figure 4d). Taken together, these data indicated that *P. gingivalis* can cause a neutrophils-dominated pro-inflammatory response in PC mice, which contributes to a suppressed tumor immune environment.

P. gingivalis recruits tumor associated-neutrophils by eliciting chemokine to promote PC

We next deeply investigated the molecular mechanisms of *P. gingivalis* in inducing an inflammatory TME. Consistent with the tumor immune landscape above, the GO terms indicated that *P. gingivalis* specifically downregulated the immune marker genes in lymphocyte chemotaxis (*Ccl12, Ccl9, Ccl8*), defense response to gram-negative bacterium (*Reg3b, Tlr5, Cd4*, App,*Mmp7*, etc.) and cytosis-related genes (*Gzme, Gzme, Gzmd, Gzmg, Gzmf*), while upregulated the genes associated with inflammatory response and neutrophil chemotaxis (*Cxcl1, Cxcl2, Cxcr2, S100a8, S100a9, Il17f*, etc.) (Figure 5a). Quantitative real-time PCR (qPCR) assay (Figure 5b) confirmed elevated expression of tumor-associated neutrophil (TAN) chemotaxis of *Cxcl1* (p= .042), *Cxcl2* (p= .048), *Cxcr2* (p= .002), *S100a8* (p= .014), *S100a9* (p= .011). Thus, we hypothesized that *P. gingivalis* induces TAN infiltration via secreting neutrophils' chemokines to promote PC progression. To test this, we blocked neutrophils' recruitment with chemokine receptor CXCR2 antagonist in *P. gingivalis*-infected subcutaneous PC model. Indeed, the pro-tumorigenesis could be markedly attenuated by chemokine blockade (p< 0.05, Figure 5c,d). A significantly decrease in neutrophils' infiltration was observed after CXCR2 antagonist treated, as evidenced by lymphocyte antigen 6 complex locus G6D+ (Ly6G+) and MPO+ cells (*p < 0.05*, Sup Figure S5).

Altogether, *P. gingivalis* induced-TANs did contribute to PC tumorigenesis, and this effect requires neutrophils' chemokines.

P. gingivalis enhances the secretion of neutrophils elastase from tumor associated-neutrophils to promote PC

Neutrophils elastase (NE), one of the main components of neutrophil extracellular traps (NETs), was recently reported to facilitate cancer progression.[23,25] Given the results of *P. gingivalis*-induced neutrophil infiltration, we then hypothesized that the releasing of NE and tumorigenesis were also enhanced in response to *P. gingivalis* infection. As expected, we found the co-expression of NE with the NET components MPO via immunofluorescence staining, and the NE released neutrophils were markedly increased in *P. gingivalis* infected PC mice than control mice (NE+cells/field: 691.4 ± 378.9 vs 63.1 ± 57.9, p< 0.001, Figure 6a,b). qPCR assay confirmed the elevated expression of NE and MPO in *P. gingivalis*-treated mice (Figure 6c). To further verify the role of NE interaction in PC tumorigenesis, we blocked NE by injection mice intraperitoneally (*i.p*) with NE inhibitor in orthotopic PC mice model (Figure 6d, *i.p* daily for 3 weeks). As expected, NE inhibitor significantly reduced tumor burden induced by *P. gingivalis* in mice (Figure 6e,f), with a significantly reduced infiltration of neutrophils as well as reversed increase of cytotoxicity T cells (p< 0.05, Sup Figure S6). Collectively, our findings illustrated the underlying role of NE in *P. gingivalis*-mediated PC tumors.

Discussion

There is a growing appreciation of the bacterial influence on tumor, with emerging evidence of the intratumor microbiome and crosstalk with the tumor biology.[26,27] Metagenomic profiling of saliva and epidemical risk analysis revealed that *P. gingivalis*, a pathogen of periodontitis, is an oncogenic bacterial candidate in PC. However, its causative role interacting between periodontitis and PC, and the underlining mechanism in promoting PC oncogenesis remain elusive. Here, we fully dissected the ecology of intratumor
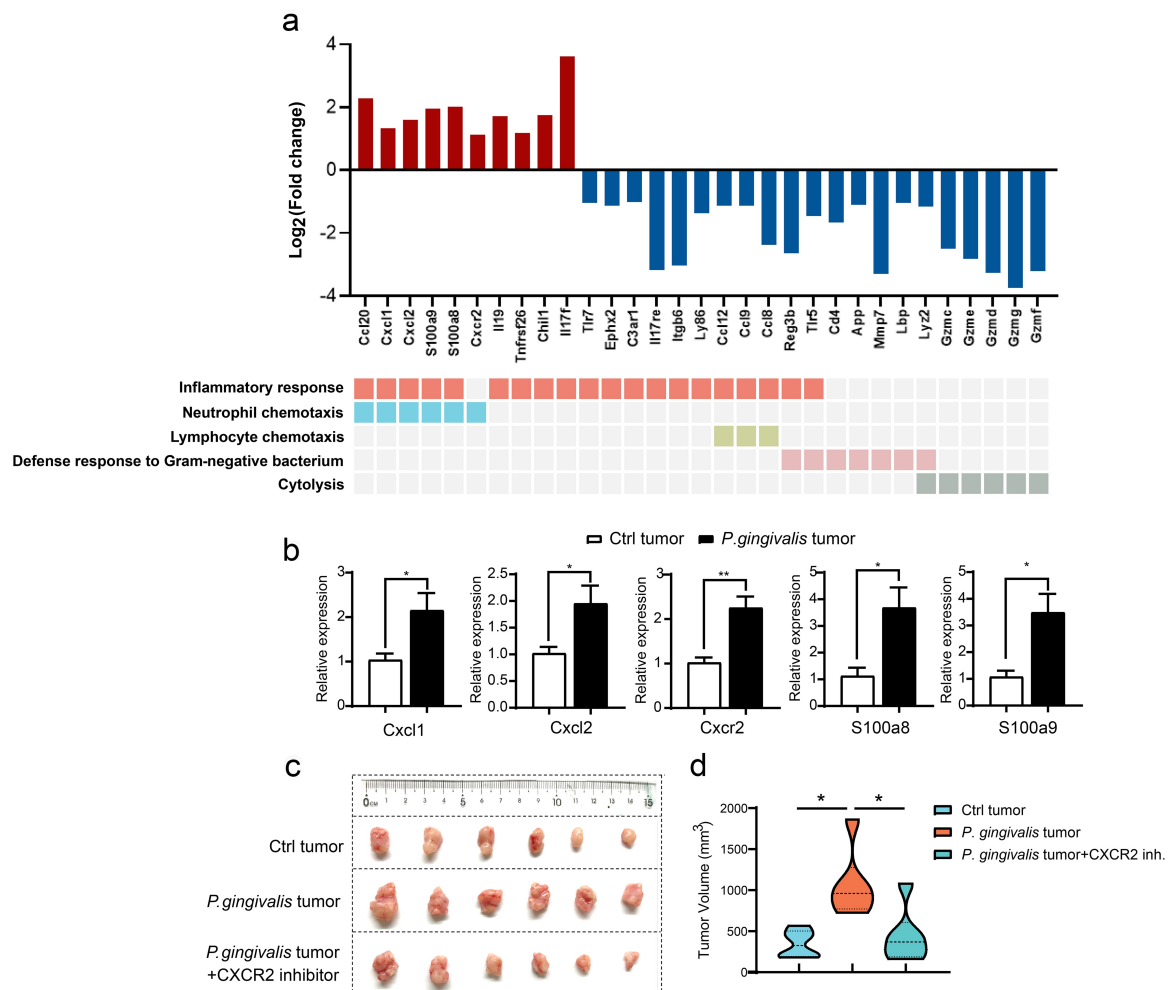
Figure 5. *P. gingivalis* enhances neutrophil chemokines' secretion to promote pancreatic cancer. (a) Bar plots of the selected ten upregulated (red) and 21 downregulated (blue) DEGs, targeting enriched gene ontology (GO) terms including inflammatory response, neutrophil chemotaxis, lymphocyte chemotaxis, defense response to gram-negative bacterium, and cytosis. (b) Quantitative real-time PCR (qPCR) validation of the upregulated genes of tumor-associated neutrophils (TAN) (*Cxcl1, Cxcl2, Cxcr2, S100a8, S100a9*) in mice tumor tissues (n = 5). (c)-(d) *P. gingivalis*- infected subcutaneous PC mice model, with or without CXCR2 inhibitors. A mixture of 3×10^5 Pan02 cells and *P. gingivalis* (MOI-100) was subcutaneously implanted into C57BL/6 mice, and 5 mg/kg CXCR2 antagonist or PBS was intraperitoneal (*i.p.*) injected every day after tumor implanted. N = 6/group. Representative *in situ* images of PC tumors are shown in (c), the tumor volume was calculated in (d). CXCR2 inh., CXCR2 inhibitor. Data shown are representative of independent experiment done with repeated 3 times, presented as mean ± SEM, *p* values were determined by two-tailed unpaired *t*-test (*$p < .05$, **$p < .01$).

microbiota in PC patients, and discovered the sharing of bacterial composition in saliva and cancerous pancreas, including *P. gingivalis*. We further demonstrated the oral-derived migration of *P. gingivalis* in the pancreas and the oncogenic potential of *P. gingivalis* in the PC. The mechanism lies in that *P. gingivalis* recruits neutrophils' accumulation and elicits NE's secretion, which ultimately promotes pancreatic neoplasms. Our findings set the stage for functional investigation of *P. gingivalis*-related cancers defined by epidemiological studies of the correlation between periodontitis and diseases.

Once considered as aseptic tumors,[28] increasing studies have now gradually established the ecology presence of microbiota within tumors.[27] Notably, several research groups independently observed that microorganisms inhabit the cancerous pancreas.[17,19,29] Here, we verified the abundance of intratumor microbiota in pancreatic cancer, and conducted a comparative analysis between the oral cavity and cancerous pancreas by performing 16s rRNA sequencing. Consistent with previous studies, similar microbial communities at various taxonomic levels and non-significantly α/β diversity were found between PC tumor tissues and their
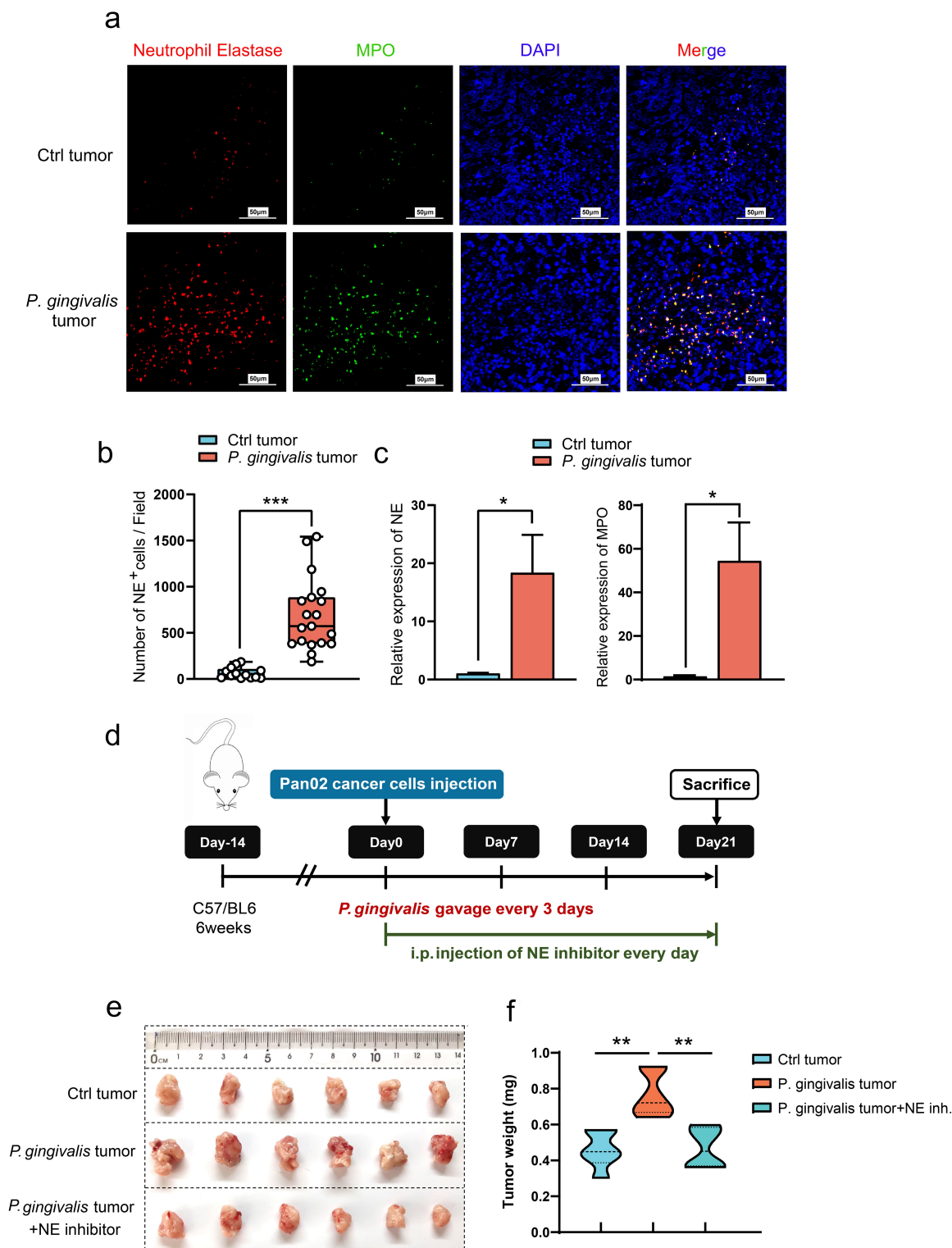
Figure 6. *P. gingivalis* enhances neutrophil elastase's secretion from tumor-associated neutrophils to promote pancreatic cancer. (a) Representative immunofluorescence analyses of neutrophil elastase (NE, red) and co-expression with MPO (green) in *P. gingivalis* or vehicle-gavaged orthotopic PC mice models. (b) Quantification of NE-positive cells per microscopic field in (a) (n = 5 mice, at least three random fields were selected, mean ± SEM, 200×). (c) qPCR validation of the expression of NE and MPO in PC tumor tissues (n = 5 mice). (d) Schematic diagram of orthotopically Pan02 cells-implanted mice model with *P. gingivalis*-gavage, treated with or without NE inhibitors. 5 mg/kg NE inhibitors or PBS were *i.p.* injected daily after the tumors were implanted. (e)-(f) Representative *in situ* images of PC tumors are shown in (e), the tumor weight was calculated in (f), sacrificed at d 21. NE blocking experiments were done with repeated three times. NE inh., NE inhibitors. *p* Values were determined by two-tailed unpaired *t*-test (*$p < 0.05$, **$p < 0.01$, ***$p < 0.001$).

NATs,[19,30] where *gammaproteobacteria* is the most enriched class, which is reported to be closely associated with chemotherapeutic drug resistance in pancreatic cancer.[29] To extend our understanding of the relationship between common clinical indicators and the intratumor microbiota community, further analysis was performed in PC tissues. *Herbaspirillum*, *Brucella* and *Allorhizobium–Neorhizobium–Pararhizobium–Rhizobium* are significantly enriched in never smokers and patients with moderately differentiated pathology, while *Treponema*, *Pseudorhodoplanes* and *Sphingomnas* were most enriched in CA19-9 normal and early-stage PC patients. This landscape study suggested the microbiome as the potential clinical predictors, though more samples are needed to validate the predictive efficacy.

Recent studies have demonstrated the retrograde bacterial migration from the gut to the pancreas[17,29,31]; here we hypothesized the possible oral-derived bacterial crosstalk. 16s rRNA sequencing was performed on newly enrolled 21 saliva samples of PC patients, compared with cancerous pancreas tissues. Despite the markedly different disposition of bacterial communities among PC tissue and saliva, we demonstrated the first time that some bacterial taxa found in the tumoral milieu were commonly present in the oral microbiome, suggesting the potentially bacterial translocation from the oral cavity to pancreas. Surprisingly, the keystone periodontitis pathogen *P. gingivalis*, usually colonized in the oral cavity, here was detected both in oral, cancerous tissues and NAT of PC patients. Although *P. gingivalis* was detected in low relative abundance, its close epidemic relationship to PC drove our attention. And thus *P. gingivalis* strain W83, one of the strains considered as virulent pathogens of periodontitis, was selected to establish mice models. When using the living cell dye calcein-AM to investigate the migration route of *P. gingivalis* via oral gavage in mice, we found the alive *P. gingivalis'* deposition both in the pancreas and feces compared with un-gavaged mice, which confirmed the potential existence of oral-gut-pancreas translocation route, though the intensity of calcein-AM (non-covalent binding dye) was decreased after a two-weeks gavaging procedure. Recent studies demonstrated the colonization of

P. gingivalis within colorectal tumors in oral-gavaged mice,[7] here our studies extending the disposition of this bacterium in PC murine model by FISH. A strength of our study is that we externally validated in 26 human PC FFPE samples, where *P. gingivalis* was significantly more enriched in the cancerous pancreas than NAT, possibly lie in the chemotactic responses of anaerobes to anaerobic conditions.[32,33] In which anaerobes like *P. gingivalis* may proliferate, as a recent study has proved the cultivation of anaerobes in pancreatic cystic neoplasms.[34] Though we could detect the *P. gingivalis'* deposition based on 16s rRNA sequencing and FISH, since the pretty low abundance of *P. gingivalis* and the relative low sensitivity of quantitative PCR assay (qPCR), we did not detect the presence of *P. gingivalis* through qPCR[35] in our present human PC samples (data not shown), more PC samples may need to confirm the methodology of qPCR in the future. Previous studies have proposed several routes of bacterial colonization to the pancreas, such as oral route, via translocation from lower gastrointestinal tract or mesenteric lymph nodes,[17,28] here we extending the potential evidences of oral–gut–pancreas route. Collectively, the 16s rRNA sequencing analysis and FISH detections showed the abundance of bacteria within the cancerous pancreas, and provided the evidence that *P. gingivalis* could migrate from oral and specifically "inoculated" in PC tissues.

Recent evidence implicates that oral microbial dysbiosis contributes to gastrointestinal cancers carcinogenesis.[5,9,26] Persistent exposure to the periodontal bacterium *P. gingivalis* could promote oncogenesis in orodigestive cancer,[36] esophageal cancer[11] and colorectal cancer[7] through the possible "mouth–gut" axis. The potential oncogenesis of *P. gingivalis* in PC has only recently begun to clarify. *P. gingivalis* was reported to promote tumorigenesis in spontaneous PC mouse models,[37] here we confirmed its pro-oncogenesis role in orthotopic and subcutaneous PC murine models, with regard to both tumor size and the activated expression of Ki67. *Gnanasekaran* et al. demonstrated that *P. gingivalis* directly improved the proliferation of PC cell lines, which could be enhanced by hypoxia.[38] However, in our *in vitro* co-culture experiments, we only found markedly proliferation

in the early stage within 24 hours, and the cell viability of PC cells was even slightly decreased with the time increase (Sup Figure S6), this may attribute to the difference in culture conditions and the toxicity of released lipopolysaccharide (LPS).[39] And thus, we speculated the potential indirect interaction between *P. gingivalis* and PC progression, based on our obvious stimulation of tumor growth *in vivo*.

P. gingivalis employs several virulence factors, driving immune escape by not only directly affecting cell signaling mechanisms but also indirectly dampening host immunity and altering cytokine production.[40] Chronic inflammation has been accounted as one of the hallmarks of tumor, whereby *P. gingivalis* shapes the proinflammatory tumor microenvironments has been reported in several cancer types.[36] Although epidemiological studies revealed a high incidence of PC in the population with periodontitis, the evidence regarding the connection of *P. gingivalis*-mediated inflammation and PC development is lacking. In our study, we observed a significant increase in neutrophils, and a decrease of CD8+ T cells in the pancreatic tumor sites compared with those of uninfected mice, such immune-suppressive TME was reported to be positively associated with tumor immune escape and reduced immunotherapeutic responses.[41] RNA sequencing unraveled that *P. gingivalis* could clearly shape the host immune responses. We noticed a strong elevation of neutrophil chemokines (*Cxcl1, Cxcl2, Cxcr2,* etc.) after *P. gingivalis* infection, while the genes related to the defense of gram-negative bacterium and antitumorigenic functions including lymphocyte chemotaxis, cell cytosis were downregulated. Generally, neutrophils always infiltrate at infected sites in many types of bacterial infections,[42] some of them are involved in close interaction with oncogenic inflammatory TME.[7,43] Here we also found neutrophils' dominant inflammatory states in *P. gingivalis* infected PC, but whether there are other potential pathogens caused the same effects needs further investigation. Collectively, these data indicate that *P. gingivalis* especially escapes from the host immune defense and strongly impairs the host anti-tumor immunity in PC mouse models.

Neutrophils, once known as the first line of immune defense against infection, are now recognized to play a key role in both initiation and progression of tumors.[44,45] In most human tumors, high infiltration of neutrophils is closely associated with adverse prognosis.[41] In the tumor microenvironment, neutrophils are recruited and turn into TANs, functionally classified as antitumorigenic N1 or pro-tumorigenic N2 phenotype.[46] We here illustrated that *P. gingivalis*-induced neutrophils in PC are mainly pro-tumor N2 subset, because they specifically over-expressed *S100a8* and *S100a9*.[47,48] We further found these TAN-promoted tumorigeneses could be reversed in *P. gingivalis*-infected mice, when CXCR2 antagonists were applied to block the neutrophils' recruiting.[20] These data indicated the indispensable role of TAN in PC progression. NE was reported to be closely associated with tumorigenesis in several cancer types, always as a complex of NET,[49-51] including pancreatic cancer.[52] As we have illustrated the intratumor *P. gingivalis* could promote PC oncogenesis, but whether it enhances NE secretion is unclear. Our results showed that the NET-associated proteases, including NE and MPO, were colocalized and significantly elevated following *P. gingivalis* infection, although the mechanisms are still needed to be illustrated. After a therapeutic NE blocking in *P. gingivalis* gavaged PC mice, we found remarkable protection against PC progression, accompanied by a significant decrease of TANs' recruitment and recovery of the infiltration of CD8+ T cells. Collectively, we here demonstrated for the first time that *P. gingivalis* from the oral cavity promote PC progression via recruiting an abundant TANs' infiltration and elevated NE secretion.

In summary, the ecology of pancreatic cancer microbiota composition, inflammation status after *P. gingivalis* infection, and their association with PC oncogenesis are recorded. Here, we verified an abundant intratumor microbiota composition in human PC tissue, among which the bacterium *P. gingivalis* from the oral cavity colonized and enriched in tumor tissue. *P. gingivalis* could induce a pro-inflammatory TME with an elevation of NE, which ultimately promotes PC progression. Our study shed new light on the connotation of the *P. gingivalis*–inflammatory system–pancreas axis in PC progression, suggesting that reduction of

P. gingivalis infections or inflammatory status could benefit PC prevention and treatment. The present study might provide preliminary data to support the epidemiological observation of the high incidence of periodontitis in PC patients. Since our study has not investigated the direct mechanism between *P. gingivalis* and the disordered inflammatory status in PC, future works are needed to explore the molecular signaling pathways in proinflammation. Besides, whether *P. gingivalis* mediates NE-dependent tumor progression in other tumor types should be expanded in future researches.

Materials and methods

Patients and specimen collection

Resected surgical tumor tissues and paired-normal adjacent tissues (NAT, n = 20) samples from PC patients were collected from Cancer Hospital, Chinese Academy of Medical Sciences. To compare the bacterial structures between intratumor and oral cavity, 21 saliva samples of PC patients were enrolled from Beijing Chaoyang Hospital, with matched age, gender and periodontal disease. Sterile surgical samples and saliva specimens were freshly collected and quickly frozen at −80°C for further high-throughput 16s rRNA gene amplicon sequencing. For FISH validation of *P. gingivalis*, FFPE samples of tumor tissues and NAT from PC patients were enrolled from Cancer Hospital, Chinese Academy of Medical Sciences. The study obtained written-informed consent from all patients and was approved by the Ethics Committee of Cancer Hospital Chinese Academy of Medical Sciences.

16S rRNA sequencing and bioinformatics analysis

Bacterial genomic DNA was extracted from surgical tissues and saliva specimens using E.Z.N.A. ® DNA Extraction Kit (Omega Biotek, USA) according to the manufacturer's instructions. The 16s rRNA gene sequencing was performed at Shanghai Majorbio Bio-pharm Technology (China) according to the standard procedures. Briefly, 16s rRNA V3-V4 region was amplified by PCR (Primers were listed in Sup Table S5).

The DNA sequencing libraries were performed on the Illumina Miseq and Ion S5 XL platform. fastp Software was used for quality control of the original sequencing sequence, and Fast Length Adjustment of SHort reads (FLASH) software was used for splicing, with the following criteria: the 300 bp reads were truncated at any site receiving an average quality score of <20 over a 50 bp sliding window, and the truncated reads shorter than 50 bp were discarded, reads containing ambiguous characters were also discarded.[53] The operational taxonomic units (OTUs) clustering of sequences are based on 97% similarity and elimination of chimeras. RDP classifer (http://rdp.cme.msu.edu/) was used to compare each sequence with the Silva database (SSU132), the alignment threshold was set to 70%, and the results of species classification annotation are obtained.

The data were analyzed by R software (Version 3.6.1) or on the free online platform of Majorbio Cloud Platform. The differential abundance analysis at different levels were performed using R, the OTU tables were analyzed but excluded the norank and unclassified taxa. The significant differentially genera in cancer and normal groups were determined by the Wilcoxon Signed-rank test ($p < 0.05$). The hierarchically clustered heatmaps were carried out based on Pearson correlation coefficients. Volcano plotted were analyzed by DESeq2 package in R, a two-sided Wald test was used, and the Y-axis was inversed with log version, along with a Benjamini–Hochberg FDR q-value. The X-axis showed the significantly two folds-increased or decreased genus, inversed with log version. Bacteria α diversity was calculated using the following index: ace, sobs, chao, shonnon and simpson. Wilcoxon Signed-rank test was used for statistical testing of two group comparisons. β Diversity analysis utilized vegan package in R, the principal co-ordinates analysis (PCoA) analyzed based on Bray–Curtis distance.

Fluorescent in situ hybridization (FISH)

P. gingivalis FAM-conjugated POGI probe (CAATACTCGTATCGCCCGTTATTC)[54] was labeled with Spectrum-Green, A Cy5-conjugated EUB338

universal bacterial probe[55] (GCTGCCTCCCG TAGGAGT) was labeled with Spectrum-Red (Thermo Fisher Scientific), as the positive control. FISH was performed according to the manufacturer's instructions. Fluorescence microscopic analysis was conducted with the confocal microscope.

Bacteria strains and cell lines

P. gingivalis (ATCC BAA-308, W83) stains were purchased from ATCC. The culture conditions of *P. gingivalis* were performed as previously described with slight alteration.[7,35] *P. gingivalis* grew on tryptic soy broth (TSB) blood agar plates supplemented with vitamin K (1 μg/mL), hemin (5 μg/mL), and sterilized sheep blood (5%) under anaerobic conditions at 37°C for 5–7 days. The monoclonal colonies were then picked up and inoculated in sterilized BHI (Brain Heart Infusion) medium with vitamin K (1 μg/mL) and hemin (5 μg/mL) until the mid-logarithmic growth phase.

Murine pancreatic cancer cell line Pan02 was purchased from Beina Chuanglian Biotechnology Research Institute (Beijing, China). These cells were cultured in a humidified 5% CO_2 atmosphere at 37°C and incubated in RPMI 1640 containing 10% fetal bovine serum (Gibco, CA).

Mouse models

Six-week male C57/BL6 mice (18–20 g) were included, ordered from Beijing Huafukang Bioscience Co. Inc (China), maintained in a barrier facility at the Cancer Hospital Chinese Academy of Medical Sciences (Beijing, China). All animal procedures were approved and conducted in accordance with Institutional Animal Care guidelines.

In *P. gingivalis*-gavaged orthotopic PC model, C57/BL6 mice were coded and randomly divided into two groups (n = 10, 5 mice/group): the *P. gingivalis*-treated group, *P. gingivalis* was suspended in at a dose of 3×10^9 CFU in 100 μL 2% carboxymethyl cellulose (CMC) and gavaged to each mice every 3 d, last for 5 weeks; the control group, mice were gavaged with 100 μL 2% CMC only. The orthotopic pancreatic cancer model was generated in C57/BL6 mice in the third week, as described previously.[33] Briefly, 50 μL Pan02 cells (3×10^5

cells) solution in PBS was injected into the head of the pancreas through a 1 cm incision in the left upper abdomen, after being anesthetized with sodium pentobarbital (40 mg/kg). When the biggest tumor's size approached about 1 cm (approximately 21 d after being inoculated), the mice were euthanized, the tumors were dissected. For NE blocking therapy in *P. gingivalis*-gavaged orthotopic PC model, mice were randomly divided into three groups (n = 18, 6 mice/group): the NE-treated group, NE inhibitor (Oct-35, Ambient, 5 mg/kg) was injected intraperitoneally (*i.p.*) daily after the tumor cell inoculated,[56] the control mice and *P. gingivalis*-gavaged mice were *i.p.* injected with vehicle (1% DMSO in PBS). In *P. gingivalis*-infected subcutaneous PC model, a mixture of 2.5×10^5 Pan02 cells and *P. gingivalis* (MOI = 100) in PBS was subcutaneously inoculated into the right flank of mice, then were randomly divided into three groups (n = 18, 6 mice/group). For CXCR2 inhibitor therapy in the subcutaneous PC model, CXCR2 antagonist (SB225002, Selleck, 5 mg/kg) or vehicle (1% DMSO in PBS) was *i.p.* injected daily throughout the experiment.[57,58] The inhibitors above were injected blindly by different researchers, and all the murine experiments were repeated at least three times.

Histologic analysis and immunohistochemistry

Tissues were fixed in 4% paraformaldehyde, embedded in paraffin and sectioned at 4-μm thickness. Then deparaffinized in xylene and rehydrated in graded ethanol, and stained with hematoxylin and eosin (H&E) using routine protocols, then reviewed in a blinded manner by experienced pathologists. The percentage of the necrotic area[59] was calculated by ImageJ, fields of each slide were randomly selected.

FFPE tumor sections were processed as described above, and then treated with antigen retrieval solution (Tris/EDTA pH 9.0). After unspecific sites blocking with 5% BSA, tissues were stained with primary anti-Ki67 (1:400, #12202, CST), anti-MPO (1:1000, ab188211, Abcam) or anti-Ly6G (1:1000, ab238132, Abcam). Secondary antibody was used and developed with 3,3′diamino benzidine (DAB) and counterstained with hematoxylin. The Ki67 index was determined by counting the proportion of Ki67 positive cells by Image-Pro Plus (version 4.5,

USA), at least three random microscopic fields of each slide were counted. The H-score of MPO was measured based on Image J (IHC profiters plugins), at least three random fields were selected. H-score = (1× weakly stained cells) + (2× moderately stained cells) + (3× strongly stained cells). The cell counts of Ly6G$^+$ or MPO$^+$ cells were recorded as positive cells/per field based on Image-Pro Plus (version 4.5, USA), at least four random microscopic fields of each slide were counted.

Flow cytometry

Fresh pancreatic cancer tissues were harvested from mice, incubated in PBS solution with 400 U/mL collagenase IV (Sorlabio, C8160) and 50 mg/mL DNase I for 30 min at 37°C on an incubator shaker following dissection. The digested tumors were filtered through 70 μm cell strainers. Cells were incubated with fluorochrome-conjugated monoclonal antibodies of murine cell surfaces markers (anti-CD45 PE-cy7, anti-CD3e APC-cy7, anti-CD4-FITC, anti-CD8-PE, anti-CD11b-APC, from BioLegend, anti- Ly6G-PerCP cy5.5 from BD). Flow cytometry was performed in BD LSRII, and data were analyzed by Flowjo v.10 software (USA).

RNA sequencing and qPCR analysis

Tumor tissues of mice were harvested, after washing with PBS, total RNA was extracted with TRIzol reagent (Thermo Fisher Scientific). Then, high-throughput RNA-sequencing was performed by Novogene Technology (Beijing, China). The obtained differentially expressed genes (DEG) ($p < 0.05$ in one-tailed unpaired t-test, and absolute fold change >2) were analyzed by Gene Ontology (GO) functional annotation and enrichment.

Reverse transcription was performed using reverse transcription reagents (RR047A, Takara). Ten microliters of reaction mix contained 2× Power SYBR Green master mix (RR420A, Takara), 100 nmol/L of forward and reverse primers (Sup Table S5), and 15 ng sample cDNA on the QIAGEN Rotor-Gene Q Real-time PCR instrument. The reaction was programmed as follows: 30 s at 95°C, 40 cycles of 5 s at 95°C and 30 s at 60°C.

Immunofluorescence staining

FFPE tumor sections were processed as described above. Antigen retrieval was performed using citrate buffer (PH = 6.0). Primary antibodies used were as follows: rabbit anti-mouse NE (1:100, BS-6982 R, Bioss), rabbit anti-mouse MPO (1:1000, ab188211, Abcam). The primary antibodies were detected with FITC (ZF-0311, ZhongShanJinQiao Co., LTD) or Cy5 (ab6564, Abcam) conjugated goat anti-rabbit IgG, respectively. Then, DAPI was used for counterstaining the nuclei, and images were obtained by laser scanning confocal microscopy. The number of NE positive cells was counted by Image-Pro Plus (version 4.5, USA).

Statistical analysis

Statistical analysis was performed using SPSS 17.0 and GraphPad Prism 8 (GraphPad Software, Inc.). Data were expressed as mean ± SD of three repeating experiments. The difference in measurement data between the two groups was assessed using a two-tailed/one-tailed Student t test (assumptions of homogeneity of variance using Levene test underlie this test) and Wilcoxon signed rank test. P values less than 0.05 were considered statistically significant.

Authors' contributions

J.M and W.Y designed the research, Q.T and X.M performed the research, analyzed the data and wrote the manuscript. Y.B. X collected the pancreatic cancer tissue and saliva samples. B. Y, Y.L and X.J.W analyzed the data. All authors contributed to the article and approved the submitted version.

Data availability statement

The datasets generated during and/or analyzed during the current study are available from the corresponding author on reasonable request. The raw fastq sequences generated from the 16S amplicon sequencing and RNA sequencing are available in the National Center for Biotechnology Information (NCBI) via the project number PRJNA804264 (https://www.ncbi.nlm.nih. gov/sra/PRJNA804264) and PRJNA804408 (https://www.ncbi. nlm.nih.gov/sra/PRJNA804408).

Ethics approval

The study was approved by the Ethics Committee of Cancer Hospital Chinese Academy of Medical Sciences (No. 17-168/ 1424). All animal procedures were approved (No. 21/290-2961) and conducted in accordance with Institutional Animal Care guidelines.

References

1. Siegel RL, Miller KD, Jemal A. Cancer statistics. CA Cancer J Clin. 2018;68(1):7–30. doi:10.3322/caac.21442.
2. Rawla P, Sunkara T, Gaduputi V. Epidemiology of pancreatic cancer: global trends, etiology and risk factors. World J Oncol. 2019;10(1):10–27. doi:10.14740/wjon1166.
3. Bascones-Martínez A, González-Febles J, Sanz-Esporrín J. Diabetes and periodontal disease. Review of the literature. Am J Dent. 2014;27:63–67.
4. Lockhart PB, Bolger AF, Papapanou PN, Osinbowale O, Trevisan M, Levison ME, Taubert KA, Newburger JW, Gornik HL, Gewitz MH, Wilson WR. Periodontal disease and atherosclerotic vascular disease: does the evidence support an independent association?: a scientific statement from the American Heart Association. Circ. 2012;125 (20):2520–2544. doi:10.1161/CIR.0b013e31825719f3.
5. Fitzpatrick SG, Katz J. The association between periodontal disease and cancer: a review of the literature. J Dent. 2010;38(2):83–95. doi:10.1016/j.jdent.2009.10.007.
6. Kitamoto S, Nagao-Kitamoto H, Hein R, Schmidt TM, Kamada N. The bacterial connection between the oral cavity and the gut diseases. J Dent Res. 2020;99 (9):1021–1029. doi:10.1177/0022034520924633.

7. Wang X, Jia Y, Wen L, Mu W, Wu X, Liu T, Liu X, Fang J, Luan Y, Chen P, et al. Porphyromonas gingivalis promotes colorectal carcinoma by activating the hematopoietic NLRP3 inflammasome. Cancer Res. 2021;81 (10):2745–2759. doi:10.1158/0008-5472.CAN-20-3827.
8. Maisonneuve P, Amar S, Lowenfels AB. Periodontal disease, edentulism, and pancreatic cancer: a meta-analysis. Ann Oncol Off J Eur Soc Med Oncol. 2017;28(5):985–995. doi:10.1093/annonc/mdx019.
9. Michaud DS, Fu Z, Shi J, Chung M. Periodontal disease, tooth loss, and cancer risk. Epidemiol Rev. 2017;39 (1):49–58. doi:10.1093/epirev/mxx006.
10. Reitano E, De'angelis N, Gavriilidis P, Gaiani F, Memeo R, Inchingolo R, Bianchi G, de'Angelis GL, Carra MC. Oral bacterial microbiota in digestive cancer patients: a systematic review. Microorganisms. 2021;9(12):2585. doi:10.3390/microorganisms9122585.
11. Peters BA, Wu J, Pei Z, Yang L, Purdue MP, Freedman ND, Chang H, Geese WJ, Paz-Ares L, Carbone DP. Oral microbiome composition reflects prospective risk for esophageal cancers. Cancer Res. 2017;77 (23):6777–6787. doi:10.1158/0008-5472.CAN-17-1296.
12. Fan X, Alekseyenko AV, Wu J, Peters BA, Jacobs EJ, Gapstur SM. Human oral microbiome and prospective risk for pancreatic cancer: a population-based nested case-control study. Gut. 2018;67(1):120–127. doi:10.1136/gutjnl-2016-312580.
13. Karpiński TM. The microbiota and pancreatic cancer. Gastroenterol Clin North Am. 2019;48(3):447–464. doi:10.1016/j.gtc.2019.04.008.
14. Stasiewicz M, Kwaśniewski M, Karpiński TM. Microbial associations with pancreatic cancer: a new frontier in biomarkers. Cancers. 2021;14(1):13. doi:10.3390/cancers14010013.
15. Wong-Rolle A, Wei HK, Zhao C, Jin C. Unexpected guests in the tumor microenvironment: microbiome in cancer. Protein Cell. 2021;12(5):426–435. doi:10.1007/s13238-020-00813-8.
16. McAllister F, Khan MAW, Helmink B, Wargo JA. The tumor microbiome in pancreatic cancer: bacteria and beyond. Cancer Cell. 2019;36(6):577–579. doi:10.1016/j.ccell.2019.11.004.
17. Pushalkar S, Hundeyin M, Daley D, Zambirinis CP, Kurz E, Mishra A, Mohan N, Aykut B, Usyk M, Torres LE. The pancreatic cancer microbiome promotes oncogenesis by induction of innate and adaptive immune suppression. Cancer Discov. 2018;8 (4):403–416. doi:10.1158/2159-8290.CD-17-1134.
18. Sethi V, Kurtom S, Tarique M, Lavania S, Malchiodi Z, Hellmund L. Gut microbiota promotes tumor growth in mice by modulating immune response. Gastroenterology. 2018;155(1):33–7.e6. doi:10.1053/j.gastro.2018.04.001.

19. Thomas RM, Gharaibeh RZ, Gauthier J, Beveridge M, Pope JL, Guijarro MV, Yu Q, He Z, Ohland C, Newsome R. Intestinal microbiota enhances pancreatic carcinogenesis in preclinical models. Carcinogenesis. 2018;39(8):1068–1078. doi:10.1093/carcin/bgy073.

20. Ley K, Hoffman HM, Kubes P, Cassatella MA, Zychlinsky A, Hedrick CC . Neutrophils: new insights and open questions. Sci Immunol. 2018;3(30):eaat4579. doi:10.1126/sciimmunol.aat4579.

21. Darveau RP. Porphyromonas gingivalis neutrophil manipulation: risk factor for periodontitis? Trends Microbiol. 2014;22(8):428–429. doi:10.1016/j.tim.2014.06.006.

22. Sochalska M, Potempa J. Manipulation of neutrophils by porphyromonas gingivalis in the development of periodontitis. Frontiers in cellular and infection microbiology. Frontiers in Cellular and Infection Microbiology. 2017;7:197. doi:10.3389/fcimb.2017.00197.

23. Lerman I, Hammes SR. Neutrophil elastase in the tumor microenvironment. Steroids. 2018;133:96–101. doi:10.1016/j.steroids.2017.11.006.

24. Sato T, Takahashi S, Mizumoto T, Harao M, Akizuki M, Takasugi M. Neutrophil elastase and cancer. Surg Oncol. 2006;15(4):217–222. doi:10.1016/j.suronc.2007.01.003.

25. Erpenbeck L, Schön MP. Neutrophil extracellular traps: protagonists of cancer progression? Oncogene. 2017;36 (18):2483–2490. doi:10.1038/onc.2016.406.

26. Garrett WS. Cancer and the microbiota. Science (New York, N.Y.). 2015;348(6230):80–86. doi:10.1126/science.aaa4972.

27. Nejman D, Livyatan I, Fuks G, Gavert N, Zwang Y, Geller LT, Rotter-Maskowitz A, Weiser R, Mallel G, Gigi E. The human tumor microbiome is composed of tumor type-specific intracellular bacteria. Science (New York, NY). 2020;368(6494):973–980. doi:10.1126/science.aay9189.

28. Thomas RM, Jobin C. Microbiota in pancreatic health and disease: the next frontier in microbiome research. Nat Rev Gastroenterol Hepatol. 2020;17(1):53–64. doi:10.1038/s41575-019-0242-7.

29. Geller LT, Barzily-Rokni M, Danino T, Jonas OH, Shental N, Nejman D, Vallée T, Klein-Peschanski C, Viader F, De la Sayette V, et al. Potential role of intratumor bacteria in mediating tumor resistance to the chemotherapeutic drug gemcitabine. Science (New York, NY). 2017;357(6356):1156–1160. doi:10.1126/science.aah5043.

30. Riquelme E, Zhang Y, Zhang L, Montiel M, Zoltan M, Dong W, Quesada P, Sahin I, Chandra V, San Lucas A, et al. Tumor microbiome diversity and composition influence pancreatic cancer outcomes. Cell. 2019;178 (4):795–806.e12. doi:10.1016/j.cell.2019.07.008.

31. Del Castillo E, Meier R, Chung M, Koestler DC, Chen T, Paster BJ Charpentier KP, Kelsey KT, Izard J, Michaud DS. The microbiomes of pancreatic and duodenum tissue overlap and are highly subject specific but differ between pancreatic cancer and noncancer subjects. Cancer Epidemiol Biomarkers Prev. 2019;28 (2):370–383. doi:10.1158/1055-9965.EPI-18-0542.

32. Oelschlaeger TA. Bacteria as tumor therapeutics? Bioeng Bugs. 2010;1(2):146–147. doi:10.4161/bbug.1.2.11248.

33. Yu YA, Shabahang S, Timiryasova TM, Zhang Q, Beltz R, Gentschev I. Visualization of tumors and metastases in live animals with bacteria and vaccinia virus encoding light-emitting proteins. Nat Biotechnol. 2004;22(3):313–320. doi:10.1038/nbt937.

34. Halimi A, Gabarrini G, Sobkowiak MJ, Ateeb Z, Davanian H, Gaiser RA, Arnelo U, Valente R, Wong AY, Moro CF, et al. Isolation of pancreatic microbiota from cystic precursors of pancreatic cancer with intracellular growth and DNA damaging properties. Gut Microbes. 2021;13(1):1983101. doi:10.1080/19490976.2021.1983101.

35. Dominy SS, Lynch C, Ermini F, Benedyk M, Marczyk A, Konradi A, McKeegan KD. Porphyromonas gingivalis in Alzheimer's disease brains: evidence for disease causation and treatment with small-molecule inhibitors. Sci Adv. 2019;5(1):eaau3333. doi:10.1126/sciadv.aau3333.

36. Olsen I, Yilmaz Ö. Possible role of Porphyromonas gingivalis in orodigestive cancers. J Oral Microbiol. 2019;11 (1):1563410. doi:10.1080/20002297.2018.1563410.

37. Chen S-M, Hsu L-J, Lee H-L, Lin C-P, Huang S-W, Lai CJ-L, Lin CW, Chen WT, Chen YJ, Lin YC, et al. Lactobacillus attenuate the progression of pancreatic cancer promoted by porphyromonas gingivalis in K-ras(G12D) transgenic mice. Cancers. 2020;12 (12):3522. doi:10.3390/cancers12123522.

38. Gnanasekaran J, Binder Gallimidi A, Saba E, Pandi K, Eli Berchoer L, Hermano E, Angabo S, Makkawi H, Khashan A, et al. Intracellular porphyromonas gingivalis promotes the tumorigenic behavior of pancreatic carcinoma cells. Cancers. 2020;12(8):2331. doi:10.3390/cancers12082331.

39. van Langevelde P, Kwappenberg KM, Groeneveld PH, Mattie H, van Dissel JT. Antibiotic-Induced lipopolysaccharide (LPS) release from salmonella typhi: delay between killing by ceftazidime and imipenem and release of LPS. Antimicrob Agents Chemother. 1998;42(4):739–743. doi:10.1128/AAC.42.4.739.

40. Hajishengallis G, Lamont RJ. Breaking bad: manipulation of the host response by P orphyromonas gingivalis. Eur J Immunol. 2014;44(2):328–338. doi:10.1002/eji.201344202.

41. Howard R, Kanetsky PA, Egan KM. Exploring the prognostic value of the neutrophil-to-lymphocyte ratio in cancer. Sci Rep. 2019;9(1):19673. doi:10.1038/s41598-019-56218-z.

42. Zhang D, Frenette PS. Cross talk between neutrophils and the microbiota. Blood. 2019;133(20):2168–2177. doi:10.1182/blood-2018-11-844555.

43. Kostic AD, Chun E, Robertson L, Glickman JN, Gallini CA, Michaud M. Fusobacterium nucleatum potentiates intestinal tumorigenesis and modulates the tumor-immune microenvironment. Cell Host Microbe. 2013;14(2):207–215. doi:10.1016/j.chom.2013.07.007.

44. Jaillon S, Ponzetta A, Di Mitri D, Santoni A, Bonecchi R, Mantovani A. Neutrophil diversity and plasticity in tumour progression and therapy. Nat Rev Cancer. 2020;20(9):485–503. doi:10.1038/s41568-020-0281-y.

45. Nicolás-Ávila J, Adrover JM, Hidalgo A. Neutrophils in homeostasis, immunity, and cancer. Immunity. 2017;46 (1):15–28. doi:10.1016/j.immuni.2016.12.012.

46. Wang X, Qiu L, Li Z, Wang X-Y, Yi H. Understanding the multifaceted role of neutrophils in cancer and auto-immune diseases. Front Immunol. 2018;9:2456. doi:10.3389/fimmu.2018.02456.

47. Gielen PR, Schulte BM, Kers-Rebel ED, Verrijp K, Bossman SA, Ter Laan M, Wesseling P, Adema GJ. Elevated levels of polymorphonuclear myeloid-derived suppressor cells in patients with glioblastoma highly express S100A8/9 and arginase and suppress T cell function. Neuro-oncology. 2016;18(9):1253–1264. doi:10.1093/neuonc/now034.

48. Zhao F, Hoechst B, Duffy A, Gamrekelashvili J, Fioravanti S, Manns MP, Greten TF, Korangy F. S100A9 a new marker for monocytic human myeloid-derived sup-pressor cells. Immunology. 2012;136(2):176–183. doi:10.1111/j.1365-2567.2012.03566.x.

49. Albrengues J, Shields MA, Ng D, Park CG, Ambrico A, Poindexter ME, Upadhyay P, Uyeminami DL, Pommier A, Kü ttner V, et al. Neutrophil extracellular traps produced during inflammation awaken dormant cancer cells in mice. Science (New York, NY). 2018;361 (6409). doi:10.1126/science.aao4227.

50. Berger-Achituv S, Brinkmann V, Abed UA, Kühn LI, Ben-Ezra J, Elhasid R, Zychlinsky A. A proposed role for neutrophil extracellular traps in cancer immunoediting. Front Immunol. 2013;4:48. doi:10.3389/fimmu.2013.00048.

51. Yang L, Liu Q, Zhang X, Liu X, Zhou B, Chen J, Huang D, Li J, Li H, Chen F. DNA of neutrophil extra-cellular traps promotes cancer metastasis via CCDC25. Nat. 2020;583(7814):133–138. doi:10.1038/s41586-020-2394-6.

52. Miller-Ocuin JL, Liang X, Boone BA, Doerfler WR, Singhi AD, Tang D, Kang R, Lotze MT, Zeh III HJ. DNA released from neutrophil extracellular traps (NETs) activates pancreatic stellate cells and enhances pancreatic tumor growth. Oncoimmunology. 2019;8(9): e1605822–e. doi:10.1080/2162402X.2019.1605822.

53. Magoč T, Salzberg SL. FLASH: fast length adjustment of short reads to improve genome assemblies. England): Bioinformatics (Oxford; 2011. Vol. 27. p. 2957–2963.

54. Sunde PT, Olsen I, Göbel UB, Theegarten D, Winter S, Debelian GJ, Tronstad L, Moter A. Fluorescence in situ hybridization (FISH) for direct visualization of bacteria in periapical lesions of asymptomatic root-filled teeth. Vol. 149. England): Microbiology (Reading; 2003:1095–1102.

55. Long X, Wong CC, Tong L, Chu ESH, Ho Szeto C, Myy G, Coker OO, Chan AW, Chan FK, Sung JJ, et al. Peptostreptococcus anaerobius promotes colorectal car-cinogenesis and modulates tumour immunity. Nat Microbiol. 2019;4(12):2319–2330. doi:10.1038/s41564-019-0541-3.

56. Lerman I, Ma X, Seger C, Maolake A, Garcia-Hernandez ML, Rangel-Moreno J, Ackerman J, Nastiuk KL, Susiarjo M, Hammes SR. Epigenetic suppression of SERPINB1 promotes inflammation-mediated prostate cancer progression. Mol Cancer Res: MCR. 2019;17 (4):845–859. doi:10.1158/1541-7786.MCR-18-0638.

57. Kim IS, Gao Y, Welte T, Wang H, Liu J, Janghorban M, Sheng K, Niu Y, Goldstein A, Zhao N, et al. Immuno-subtyping of breast cancer reveals distinct myeloid cell profiles and immunotherapy resistance mechanisms. Nat Cell Biol. 2019;21(9):1113–1126. doi:10.1038/s41556-019-0373-7.

58. Wang L-Y, Tu Y-F, Lin Y-C, Huang -C-C. CXCL5 signaling is a shared pathway of neuroinflammation and blood-brain barrier injury contributing to white matter injury in the immature brain. J Neuroinflammation. 2016;13(1):6. doi:10.1186/s12974-015-0474-6.

59. Wang Y, Dai H, Li H, Lv H, Wang T, Fu X, Han W. Growth of human colorectal cancer SW1116 cells is inhibited by cytokine-induced killer cells. Clin Dev Immunol. 2011;2011:621414. 2011. doi:10.1155/2011/621414.